With the measured parameters for the resonances listed in Table I, the resonance-capture integral RI for natural Mo is calculated to be

$$RI = 27 \pm 2b.$$

This value includes the $1/v$ contribution (1.2b) and the contributions ($\sim$1b) from resonances at energies higher than about 1.5 keV. The latter contributions have been calculated according to formulas derived by Dresner.[19] Our calculated value for the resonance-capture integral agrees resonably well with the values $33.2 \pm 3.1b$ measured by Long,[20] and $25 \pm 1b$ measured by Kapchigashev and Popov.[21]

Using the parameters of the resonances measured in this experiment, we calculated the strength functions for the $s$- and $p$-wave resonances of Mo isotopes. As pointed out at the beginning of this section, we feel

[19] L. Dresner, J. Nucl. Energy **2**, 118 (1955); E. Kuhn and L. Dresner, *ibid.* **7**, 69 (1958).

[20] R. L. Long, Argonne National Laboratory Report No. ANL-6580 (1962), p. 32.

[21] S. P. Kapchigashev and Y. P. Popov, Soviet J. Atomic Energy **15**, 808 (1964).

that a significant fraction of the small resonances have been missed at energies greater than about 300 eV. Therefore, in calculating the $p$-wave strength functions, only that portion of the data obtained for $E_n < 300$ eV have been used. For the calculation of the $s$-wave strength function $S_0$, on the other hand, we used the parameters of all the resonances measured in this experiment, since a failure to detect or identify a weak $s$-wave resonance would not significantly influence the result. The results are shown in Table III. The errors designate 80% confidence limits calculated under the assumption that the reduced neutron width $g\Gamma_n^1$ follows the Porter-Thomas distribution. Our results agree closely with the values $S_0 \approx 0.5 \times 10^{-4}$ and $S_1 \approx 5 \times 10^{-4}$ reported previously.[1,2,15]

## ACKNOWLEDGMENTS

---

# Spins and Widths of Energy Levels in the 5–9-MeV Region*

S. Ramchandran† and J. A. McIntyre

*Texas A&M University, College Station, Texas*

(Received 15 April 1968; revised manuscript received 18 November 1968)

Neutron-capture $\gamma$ rays from the Texas A&M research reactor have been used to excite one nuclear energy level each in $^{90}$Zr, Cd, Sn, Hg, $^{205}$Tl, and $^{208}$Pb, and two in $^{209}$Bi, in the 5–9-MeV region. Angular-distribution measurements of the scattered $\gamma$ rays showed that the transitions were all consistent with dipole radiation. However, for various reasons, the data could also be reproduced in most cases by assuming a mixture of dipole and quadrupole radiation. Three further measurements were made for the $^{90}$Zr, the $^{205}$Tl, the $^{208}$Pb, and one $^{209}$Bi excitation: (1) an absolute differential cross-section measurement on the resonance scattering, (2) a resonance absorption measurement, and (3) a differential cross-section measurement at liquid-nitrogen temperature. From these data, values were found for $\Gamma_0$ (the excited level width for an electromagnetic transition to the ground state), $\Gamma$ (the excited level total electromagnetic width), and $\epsilon$ (the energy displacement between the neutron-capture $\gamma$-ray energy and the resonance energy). The values of $\Gamma_0$ (between 0.14 and 1.0 eV) were found to be about 10 times larger than the values usually found for $\gamma$-ray widths in this energy region as determined from neutron-capture reactions.

## I. INTRODUCTION

MANY properties of a nuclear energy level can be studied through the excitation of the level by the electromagnetic resonance fluorescence process. A number of techniques have been developed for exciting nuclear levels by electromagnetic radiation; one of the most recent, and still relatively unexploited, is that of

using the extremely monoenergetic neutron-capture $\gamma$ rays to excite the nucleus to be studied. The use of neutron-capture $\gamma$ rays permits, for the first time, the study of properties of energy levels in heavy nuclei at excitation energies just below the neutron threshold where the level density is high and good energy resolution is essential.

In this paper, the study of energy levels is reported using methods that have already been described in the literature. Neutron-capture $\gamma$ rays of a few eV energy resolution strike a target whose nuclei are excited by the resonance fluorescence process since the energy of the $\gamma$
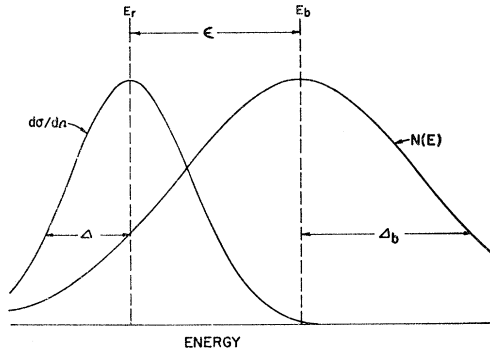
FIG. 1. Schematic representation of the scattering differential cross section $d\sigma/d\Omega$ and the $\gamma$-ray beam intensity $N(E)$ plotted against energy. Separation energy $\epsilon = |E_b - E_r|$.

rays $E_b$ lies sufficiently close to the resonance energy $E_r$ of the target nuclei.[1] The situation under consideration is illustrated in Fig. 1 where the resonance scattering differential cross section $d\sigma/d\Omega$ and the $\gamma$-ray beam intensity $N(E)$ are plotted against energy. The means of these two spectra are separated by the energy $\epsilon$. The widths of the two lines are determined primarily by the Doppler widths $\Delta$ (of the target resonance) and $\Delta_b$ (of the $\gamma$-ray beam). The amplitude of $d\sigma/d\Omega$ is a function of $\Gamma$, the total linewidth of the excited state, and $\Gamma_0$, the partial linewidth associated with the $\gamma$-ray transition to the ground state of the nucleus. The amount of resonance scattering depends on the product of $N(E)$, the beam intensity, and $d\sigma/d\Omega$, the resonance scattering cross section. Thus, a resonance scattering experiment is a function of the three parameters $\Gamma$, $\Gamma_0$, and $\epsilon$. By performing three independent experiments,[2,3] (1) an absolute scattering measurement, (2) a self-absorption measurement, and (3) a scattering measurement at low temperature (which changes the value of $\Delta$ in Fig. 1) it is possible to determine the three parameters, $\Gamma$, $\Gamma_0$, and $\epsilon$. In this paper, the results of such measurements for four nuclear excitations are reported. It should be noted that, because of the symmetries of the peaks in Fig. 1, the sign of $\epsilon$ is not determined by the

experiments. The sign of $\epsilon$ can be determined[4] by rotating the scatterer at a high velocity so that $E_r$ is changed. However, the purpose in measuring $\epsilon$ is to determine the nuclear parameters $\Gamma$ and $\Gamma_0$; thus, the sign of $\epsilon$ in this work is of no interest. In this paper, therefore, the symbol $\epsilon$ will always indicate the absolute value, $|E_b - E_r|$.

Further information about the energy level excited can be found by measuring the angular distribution of the resonance-scattered $\gamma$ rays. Such measurements give information concerning the multipolarity $L$ of the $\gamma$-ray transition and the spins $J_0$ and $J_1$ of the ground and excited states. Angular-distribution measurements were made for a total of eight nuclear levels.

Finally, in the course of investigating the elastic resonance scattering, evidence for inelastic scattering was also found for a number of the scatterers that were studied.

## II. THEORETICAL BACKGROUND

### A. Determination of the Multipolarity of the Emitted Radiation $L$ and the Spin of the Excited State $J_1$

The angular distribution of the $\gamma$ rays scattered by the resonance fluorescence process depends on the spins of the energy levels involved and the multipolarity of the radiation. The angular dependence of the scattering differential cross section $W(\theta, L, \delta, J_0, J_1)$, can be calculated using standard angular-correlation procedures.[5] Here, $\theta$ is the scattering angle, $L$ is the multipolarity of the radiation, $\delta^2 = $ (Intensity of the $L+1$ radiation)/(Intensity of the $L$ radiation), $J_0$ is the ground-state spin, and $J_1$ the excited-state spin of the nucleus. In the work to be reported here, $W(\theta)$ is measured experimentally, and $J_0$ is limited to a few values depending on the isotopes in the target. $W(\theta)$ is then calculated for various values of $L$, $\delta$, and $J_1$. Depending on the number of isotopes involved and the accuracy of the experimental data, values for $L$, $\delta$, $J_0$, and $J_1$ are then determined with various amounts of precision.

### B. Determination of $\Gamma$, $\Gamma_0$, and $\epsilon$

#### 1. General Expressions

The differential scattering cross section, $d\sigma(E)/d\Omega$ for the resonance fluorescence process can be written as

$$d\sigma(E)/d\Omega = \sigma_0(\Gamma_0/\Gamma)^2[W(\theta)/4\pi]\psi(u, v), \quad (1)$$

where

$$\sigma_0 = 2\pi\lambda^2(2J_1+1)/(2J_0+1), \quad (2)$$

$$W(\theta) = 1 + A_2{}^2(L, \delta, J_0, J_1) P_2(\cos\theta)$$

$$+ A_4{}^2(L, \delta, J_0, J_1) P_4(\cos\theta) + \cdots \quad (3)$$

[1] The important discovery that neutron-capture $\gamma$ rays will excite energy levels by resonance fluorescence was made independently by H. H. Fleischmann, by C. S. Young and D. J. Donahue, and by G. Ben-David and B. Huebschmann. The first report of Fleischmann's work was made by H. Maier-Leibniz at the Conference on Programming and Utilization of Research Reactors, Vienna, Austria; see in Proceedings of the Conference on Programming and Utilization of Research Reactors, Vienna Austria, Vol. 3, p. 145 (unpublished). The journal paper reporting the work is H. H. Fleischmann, Ann. Physik 12, 133 (1963). A report of the Young and Donahue work is given in Bull. Am. Phys. Soc. 8, 61 (1963) while their paper is C. S. Young and D. J. Donahue, Phys. Rev. 132, 1724 (1963). The resonance studied by Young and Donahue was the 7.277-MeV level in $^{208}$Pb. This excitation has since been studied by many investigators. The report of the Ben-David and Huebshmann work appeared in Phys. Letters 3, 87 (1962).

[2] H. H. Fleischmann and F. W. Stanek, Z. Physik 175, 172 (1963).

[3] M. Giannini, P. Oliva, D. Prosperi, and S. Sciuti, Nucl. Phys. 65, 344 (1965).

[4] B. Arad, G. Ben-David, and Y. Schlesinger, Phys. Rev. 136, B370 (1964).

[5] See, e.g., L. W. Fagg and S. S. Hanna, Rev. Mod. Phys. 31, 771 (1959).

and

$$\psi(u, v) = \left(\frac{1}{4\pi v}\right)^{1/2} \int_{-\infty}^{\infty} \frac{\exp[-(u-z)^2/4v]}{1+z^2} \, dz. \quad (4)$$

The parameters not defined above are the following: $2\pi\lambda$ is the $\gamma$-ray wavelength, $\Gamma_0$ is the partial linewidth of the excited state for a $\gamma$-ray transition to the ground state. $\Gamma$ is the total linewidth of the excited state, the $A_i(L, \delta, J_0, J_1)$ coefficients are tabulated[6] functions of $\delta$, the $P_i(\cos\theta)$ are Legendre polynomials,

$$u = 2(E - E_r)/\Gamma, \quad (5)$$

$$v = (\Delta/\Gamma)^2, \quad (6)$$

with $E_r$ being the resonance energy of the excited state, while $E$ is the energy of the $\gamma$ ray being scattered, and $\Delta(T)$ the Doppler width, is expressed as

$$\Delta(T) = E_r(2kT_{\text{eff}}/Mc^2)^{1/2} \quad (7)$$

with $k$ being Boltzmann's constant, $Mc^2$ the rest energy of the nucleus being excited, and $T_{\text{eff}}$ being an effective temperature[7] which accounts for the fact that the motion of the nucleus at temperature $T$ is modified by its being bound in a solid.

While Eqs. (1)–(7) were used in all the calculations reported in this paper, it is interesting to examine the $\psi$ function under certain limiting conditions so that later, an intuitive understanding of the scattering cross section can be obtained. When $\Gamma \ll \Delta$, $\psi$ becomes the Doppler or Gauss function,

$$\psi\{(\Gamma/\Delta) \to 0\} = \pi^{1/2}(\Gamma/2\Delta) \exp\{-(E-E_r)^2/\Delta^2\}. \quad (8)$$

On the other hand, when $(E - E_r) \gg \Delta$, $\psi$ becomes the Lorentz function,

$$\psi\{[\Delta/(E-E_r)] \to 0\} = (\Gamma/2)^2/[(E-E_r)^2+(\Gamma/2)^2]. \quad (9)$$

Thus, the amplitude of the Doppler function is proportional to the linewidth $\Gamma$, while the width of the Lorentz function is proportional to this same quantity. The width of the Doppler function, however, is proportional to $\Delta$ while the Lorentz function is independent of $\Delta$.

Returning to the exact analysis, the experimental quantity measured is the yield $Y$ the number of $\gamma$ rays counted by the detector which has an efficiency $\eta$ and subtends the solid angle $d\Omega$ at the scatterer. For the scattering geometry shown in Fig. 2, the yield may be expressed as

$$Y = \int_0^{\infty} dE \, N(E) \left(\frac{d\sigma(E)}{d\Omega}\right) d\Omega \eta \int_0^{x_0} n \frac{dx}{\cos\alpha} A, \quad (10)$$
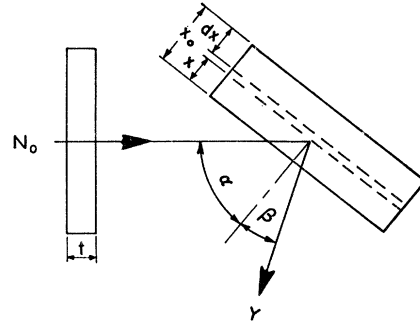


FIG. 2. Absorber and scatterer geometry.

where

$$A = \exp\{-[\mu+n\sigma_a(E)][(x/\cos\alpha)+t]\}$$

$$\times \exp[-\mu x/\cos\beta] \quad (11)$$

is the attenuation in the scatterer and the absorber. The notation is as follows: $\mu$ is the $\gamma$-ray absorption coefficient[8] excluding the resonance scattering, $n$ is the number of resonant scattering nuclei per cm³, $\sigma_a(E)$ is the resonance absorption total cross section,

$$\sigma_a(E) = \sigma_0(\Gamma_0/\Gamma)\psi(u, v), \quad (12)$$

$t$ is the thickness of the absorber in the beam before scattering occurs, while $x$, $\alpha$, and $\beta$ are defined in Fig. 2. Finally, $N(E)$ the number of $\gamma$ rays striking the target can be written as

$$N(E) = (2/\pi\Gamma_b)N_0\psi(u_b, v_b), \quad (13)$$

where $N_0$ is the number of $\gamma$ rays sec⁻¹ in the beam, $\psi$ is defined by Eq. (4), and

$$u_b = 2(E - E_b)/\Gamma_b, \quad (14)$$

$$v_b = (\Delta_b/\Gamma_b)^2. \quad (15)$$

Here, the subscript $b$ refers to parameters associated with the $\gamma$-ray beam spectrum, with $\Gamma$, $\Delta$, and $E$ being defined as before. All quantities are known in the yield expression, Eq. (10), except $\Gamma_b$, $\Gamma$, $\Gamma_0$, and $\epsilon = |E_b - E_r|$. However, $\Gamma_b$ appears only in Eqs. (10)–(13). Since $\Gamma_b$ is usually[9] about 0.1 eV while $\Delta_b$ is about 8 eV, the approximation of Eq. (8) for $\psi$ may be used and

$$N(E) = (N_0/\pi^{1/2}\Delta_b) \exp\{-(E-E_b)^2/\Delta_b^2\} \quad (16)$$

which is independent of $\Gamma_b$. Thus, the yield expression in Eq. (10) contains only the unknowns $\Gamma$, $\Gamma_0$, and $\epsilon$. [Note that the approximation of Eq. (8) is not used for $\psi$ for the excited level in the scatterer.] An IBM 7094 computer was used to calculate the yield quantities for various values of $\Gamma$, $\Gamma_0$, and $\epsilon$ using Eqs. (10)–(12) and (16). These theoretical values were then compared to

[6] See, e.g.. M. Ferentz and N. Rosenzweig, Argonne National Laboratory Report, ANL-5324 (unpublished).
[7] W. E. Lamb, Phys. Rev. **55**, 190 (1939).

[8] J. H. Hubbell and M. J. Berger, Natl. Bur. Std. (U.S.) Rept., NBS-8681 (1966); G. W. Grodstein, Natl. Bur. Std. (U.S.) Rept., NBS-583 (1957); E. Storm, E. Gilbert, and H. Israel, Los Alamos Laboratory Report, LA-2237, 1958 (unpublished).
[9] *Brookhaven National Laboratory Report No. 325* (U.S. Government Printing Office, Washington, D.C., 1958), 2nd ed.
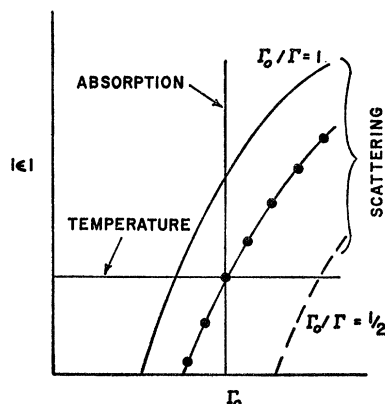
FIG. 3. Plot of the allowed values of $\Gamma_0$ and $|\epsilon|$ for the three different types of experiments: (a) absorption, (b) scattering, and (c) temperature variation. Results were obtained using the Doppler approximation of Eq. (18) and are hypothetical.

the experimental yield and a relation between $\Gamma$, $\Gamma_0$, and $\epsilon$ was thereby determined.

For purposes of planning experiments, however, it is useful to simplify the yield expression of Eq. (10) by assuming that $\Gamma \ll \Delta$ since $\Gamma$ is always less than $\Delta$ in practice. Under these conditions the $\psi$ function of Eq. (4) takes the form of Eq. (8). It will be assumed further that the absorption in the scatterer can be neglected, i.e., that $(\mu + n\sigma_a)x \ll 1$ and that the resonance absorption by the absorber is small, i.e., that $n\sigma_a t < 1$. Then, by expanding the exponential for the absorber in the manner of Ofer and Schwarzschild,[10] the yield expression of Eq. (10) can be written,

$$Y = (N_0\sigma_0/8\pi^{1/2})n\eta W(\theta)d\Omega[\Gamma_0^2/\Gamma\Delta_0(T)]$$

$$\times \exp\{-[\epsilon^2/\Delta_0^2(T)]-(\mu+c\Gamma_0)t\}x_0/\cos\alpha, \quad (17)$$

where $\Delta_0^2 = \Delta^2 + \Delta_b^2$, and $c$ is a slowly varying function of $t$. Lumping together the constants in Eq. (17), the yield expression becomes

$$Y = \text{const}[\Gamma_0^2/\Gamma\Delta_0(T)]\exp\{-[\epsilon^2/\Delta_0^8(T)]-c\Gamma_0 t\}. \quad (18)$$

The results of the different experiments can now be understood qualitatively by using Eq. (18).

### 2. Scattering Experiments

In those experiments, the yield $Y$ is measured for no absorber $(t=0)$. The variables in the yield expression [see Eq. (18)] are then $\Gamma_0^2/\Gamma$ and $\epsilon$. The procedure followed is to select a value of $\Gamma_0/\Gamma$ and then determine a curve in the $\epsilon - \Gamma_0$ plane which produces the correct value of the yield $Y$ (see Fig. 3).

### 3. Absorption Experiments

In these experiments, the yield $Y$ is measured for various values of $t$. In principle, the ratio of $Y(t=0)$

[10] S. Ofer and A. Schwarzschild, Phys. Rev. 116, 725 (1959).

and $Y(t)$ is measured. Equation (18) shows then, that $\Gamma_0$ is determined independently of $\epsilon$. Such a result is shown in Fig. 3.

The intersection of the scattering and absorption curves in Fig. 3 indicates how the two types of measurement will determine $\Gamma_0$ and put limits on $\Gamma$ and $\epsilon$. Since $\Gamma_0/\Gamma \leq 1$, the absorption line determines the minimum value allowed for $\Gamma$. Since $|\epsilon| \geq 0$, the minimum value for $\Gamma_0/\Gamma$ is determined by the scattering line intersecting the absorption line at $\epsilon = 0$. This intersection therefore determines the maximum value for $\Gamma$. It should be emphasized, however, that the analysis at this point is approximate and that an accurate analysis will give somewhat different results. However, the features displayed in Fig. 3 carry over qualitatively to the actual analysis shown in Fig. 8.

### 4. Temperature Variation Experiments

While the results of the scattering and absorption measurements can be used to put limits on the possible values for $\Gamma$, $\Gamma_0$, and $\epsilon$, a third, independent measurement is required to determine the values of these three quantities uniquely. Such a measurement is achieved by performing a scattering experiment at two different temperatures. As shown in Eq. (18), a change in the temperature of the target affects the yield through the change in $\Delta_0(T)$, where

$$\Delta_0^2(T) = \Delta^2(T) + \Delta_b^2. \quad (19)$$

Thus, if two yield measurements are made at temperatures $T_1$ and $T_2$, the ratio of the yields will be

$$Y(T_1)/Y(T_2) = [\Delta_0(T_2)/\Delta_0(T_1)]$$

$$\times \exp\epsilon^2[\Delta_0^{-2}(T_2)-\Delta_0^{-2}(T_1)]. \quad (20)$$

The temperature measurement thus determines $|\epsilon|$ and, in the approximation used, is independent of $\Gamma$ and $\Gamma_0$. The result of such a measurement is also plotted in Fig. 3. Since the temperature measurement determines $|\epsilon|$ while the absorption measurement determines $\Gamma_0$, the parameter $\Gamma$ can be obtained from the scattering measurement by selecting the correct value of $\Gamma_0/\Gamma$ to direct the scattering curve in Fig. 3 through the intersection of the absorption and temperature curves. Such a selected curve is indicated by the curve connecting the circles.

The sensitivity of the temperature measurement for determining $\epsilon$ depends on the value of $\epsilon$. For $T_1 < T_2$, and for $\epsilon \ll \Delta_0$, $Y(T_1)/Y(T_2) > 1$ in Eq. (20). However, as $\epsilon$ increases, the yield ratio decreases to values less than unity. The decrease ceases, however, as $\epsilon$ continues to grow larger until, for $\epsilon \gg \Delta_0$, the ratio increases again to unity. This increase back to unity does not occur in Eq. (20) but does occur in practice because the overlap of the spectra in Fig. 1 for $\epsilon \gg \Delta_0$ occurs only in the region of the "tails" of the $\psi$-function which have a temperature-independent Lorentz shape [see Eq. (9)]. This dependence of the yield ratio on $\epsilon$ has been calculated

for a number of different temperatures by Arad *et al.*[11] using the exact $\psi$ functions. Their results show that $\epsilon$ is determined best when $\epsilon^2 \sim \Delta_0^2(T_2) + \Delta_0^2(T_1)$.

## III. EXPERIMENTAL APPARATUS

A schematic-plane view of the apparatus is shown in Fig. 4 approximately to scale. Neutrons from the core of the 100-kW Texas A&M University research reactor are captured in the source material placed adjacent to the core. Six different source materials can be inserted by a remote drive accessible at the top of the reactor pool. The neutron flux at the position of the source is $7 \times 10^{11}$ cm$^{-2}$ sec$^{-1}$. The $\gamma$ rays produced in the $(n, \gamma)$ reactions in the source material pass through a 15-cm-diam tube placed tangentially to the reactor core. This tube traverses the pool water and abuts a larger tube through the shield wall which exits into the research area adjacent to the reactor. Such a tangential tube system yields a beam of neutron-capture $\gamma$ rays from the source material with only a small background of core neutrons and $\gamma$ rays.[12] A radial tube, on the other hand, is exposed to the direct flux from the reactor core. The beam of the $\gamma$ rays is collimated in the shield wall to a vertical slit of approximately $5 \times 10$ cm in cross section. A total of 30 cm of boron-impregnated paraffin lies in the beam path to slow down and capture neutrons passing through the pipe. The scatterer to be studied is $10 \times 10$ cm in cross section and is placed at an angle of $45°$ with respect to the beam as shown. When used, the absorber is placed in the path of the beam as indicated in Fig. 4.

The detector of the scattered $\gamma$ rays is a 7.5 cm-diam $\times 7.5$ cm-long NaI(Tl) scintillator which is surrounded by 15 cm of lead and 10 cm of paraffin impregnated with boron. A $5 \times 5$-cm aperture in the wall permits $\gamma$ rays from the scatterer to reach the scintillator. A 5-cm-thick plug of boron-impregnated paraffin is inserted in the aperture to reduce background counts from neutrons. The detector is placed on a table that can be rotated in a horizontal plane about the vertical axis through the center of the scatterer.
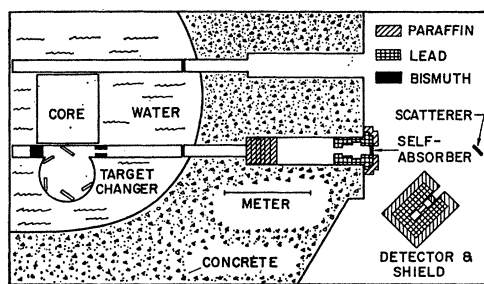


EXPERIMENTAL ARRANGEMENT

FIG. 4. Scale drawing of the experimental arrangement.

[11] B. Arad, G. Ben-David, I. Pelah, and Y. Schlesinger, Phys. Rev. **133**, B684 (1964).
[12] L. Jarczyk, H. Knoepfel, R. Müller, and W. Wölfli, Nucl. Instr. Methods **13**, 287 (1961).
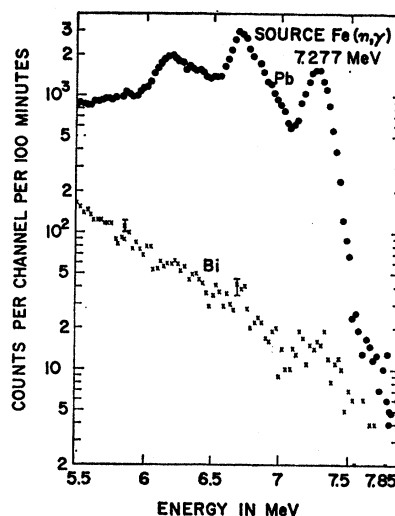


FIG. 5. Spectrum of the 7.277-MeV $\gamma$ rays resonantly scattered from Pb and the spectrum of the matched nonresonant Bi scatterer.

The relative intensity of the $\gamma$-ray beam is monitored by a Geiger counter placed 10 cm above the beam aperture at the wall of the reactor. The counts in the monitor are presumably produced by $\gamma$ rays scattered out of the beam. It was found that the ratio of the monitor counts to the reactor power level as measured by a fission chamber near the reactor core remained constant to within $1.5\%$.

## IV. EXPERIMENTAL PROCEDURE AND RESULTS

### A. Angular-Distribution Measurements

The detector was placed so that the face of the NaI(Tl) scintillator was 40 cm from the vertical axis of the target. The angle subtended by the detector in the scattering plane was $6°$. Combinations of source material at the reactor core and scatterer material at the center of the spectrometer were selected on the basis of the cross sections reported by Ben-David *et al.*[13] The pulse-height spectra of the scattered $\gamma$ rays as detected in the Na(Tl) detector were recorded by a 400-channel analyzer. One of the better spectra obtained is shown in Fig. 5, one of the poorer in Fig. 6. For the NaI(Tl) detector used, the detection of $\gamma$ rays of one energy yields a pulse-height spectrum having three peaks, as in Fig. 5. However, in Fig. 6 indications of other peaks occur at 6.95 and 4.65 MeV. The high-energy peak very likely results from resonance fluorescence excited by the 6.949-MeV $\gamma$ ray in the Co$(n, \gamma)$ spectrum. The 4.65-MeV peak could be caused by the 4.648-MeV $\gamma$ ray in the Co$(n, \gamma)$ spectrum or it may be a cascade $\gamma$ ray produced in the decay of the 6.95- or 6.485-MeV level. Such extraneous peaks were found in all but three of the spectra studied. While these peaks

[13] G. Ben-David, B. Arad, J. Balderman, and Y. Schlesinger, Phys. Rev. **146**, 852 (1966).
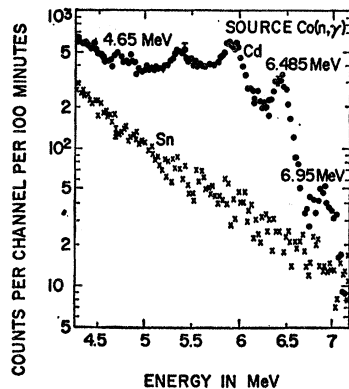
FIG. 6. Spectrum of the $\gamma$ rays scattered from Cd along with the spectrum from the matched Sn scatterer.

were not studied further, and the expected "triplet" structure was not always isolated, their positions have been listed in Table I as features worthy of further investigation. The energies of the $\gamma$ rays corresponding to the pulse-height triplets are listed in Table I. If only a doublet appears, the energy of the highest-energy peak is listed with a second energy in parenthesis which corresponds to the missing high-energy peak of the triplet. For the single 4.65-MeV peak shown in Fig. 6 a question mark is attached to the energy value listed. The utilization of Ge(Li) detectors with their high resolution will be especially helpful in future investigations of these "extra" lines as has been shown by Schlesinger, Arad, and Ben-David.[14] Also, the resolution of the Ge(Li) detectors is required in many of the cases studied here if the possibility of inelastic-scattered $\gamma$ rays being mixed in with the broad elastic scattering peaks obtained with the NaI(Tl) detector is to be eliminated. It is also possible that neutron-capture $\gamma$ rays of more than one energy might be involved in the scattering events represented by a broad NaI(Tl) peak. A number of recent measure-

TABLE I. Extraneous peaks.

| Source | Target | Energy (MeV) | Noted by other investigators |
|---|---|---|---|
| Se | Zr | 6.60 | a |
| Co | Cd | 6.95 | |
| | | 4.65(?) | |
| Cu | Sn | 5.25(5.76) | |
| Fe | Tl | 5.62 | b |
| Ti | Bi | 5.65(6.16) | |

a G. Ben-David, B. Arad, J. Balderman, and Y. Schlesinger, Phys. Rev. 146, 852 (1966).
b R. Moreh and G. Ben-Yaacov, Nuclear Research Center—Negev Report,NRCN-180, 1967 (unpublished).

[14] Y. Schlesinger, B. Arad, G. Ben-David, Israel Atomic Energy Commission Report IA-1128, 1966 (unpublished).

ments with Ge(Li) detectors have clarified the experimental situation in many cases; these data will be considered in Sec. V A when the individual excitations are discussed.

Also shown in Figs. 5 and 6 are spectra obtained from matched "dummy" scatterers which have similar electronic and gross nuclear properties as the primary scatterers. The spectrum of the resonance scattering is taken to be the difference of the spectra of the primary and of the dummy scatterers. The difference spectrum thereby obtained was in quite good agreement with published NaI(Tl) spectra for monoenergetic $\gamma$ rays.[15]

Measurements were then made of counting rate versus angle of scattering for eight resonance scattering processes. The counting rate was considered to be the number of counts lying in the two highest-energy peaks
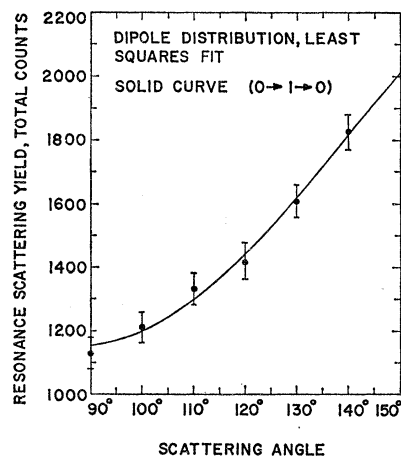


FIG. 7. Least-squares fit [assuming a $1+\alpha P_2(\cos\theta)$ distribution] to the experimental angular distribution of the 6.988-MeV $\gamma$ rays resonantly scattered from Sn using Cu$(n, \gamma)$ rays.

of the elastic scattering triplet. A typical angular distribution is shown in Fig. 7 for the case of 6.988-MeV neutron-capture $\gamma$ rays from Cu being scattered by Sn. The experimental data are the points with error bars. The curve was found by making a least-squares fit to the data with a function of the form $N[1+\alpha P_2(\cos\theta)]$, where $N$ and $\alpha$ are adjustable parameters and $P_2(\cos\theta)$ is the Legendre polynomial of second degree. This fitting procedure was carried out for all of the eight angular distributions measured; statistically good fits were obtained for all distributions. The $\alpha$ values obtained are listed in Table II in spaces corresponding to $J_0$ values consistent with the isotopes in the scatterer, and to $J_1$ values allowed for by dipole transitions. The error in the $\alpha$ value $\Delta\alpha$ was found[16] by calculating $\chi^2$ for the least-squares fit and then finding the value $\alpha+\Delta\alpha$ which increased the value of $\chi^2$ to $\chi^2+1$.

[15] L. Jarczyk, H. Knoepfel, J. Lang, R. Müller, and W. Wölfli, Nucl. Instr. Methods 17, 310 (1962).
[16] See, e.g., S. D. Baker and J. A. McIntyre, Phys. Rev. 161, 1200 (1967).

For interpreting the $\alpha$ values found, a comparison to theory must be made. This comparison is made through the usual multipole expansion. The simplest assumption is to consider only the first term in the expansion, the dipole term. If this assumption is made, the angular distribution has the form[5]:

$$W(\theta) = 1 + A_2^2(J_0, J_1, L=1) P_2(\cos\theta),$$

where $L$ is the multipolarity of the transition and $A_2$ is a tabulated function. The values[6] for $A_2^2$ are shown for various possible values of $J_0$ and $J_1$ in Table II. If the scattering is dipole, the experimental $\alpha$ value should be the same as the theoretical $A_2^2$ value. It is seen that indeed, there is always one and only one pair of $J_0$ and $J_1$ values where $A_2^2$ corresponds to the experimental parameter $\alpha$ (see the bold figures for value of $\alpha$ in the table). Thus, the angular-distribution data are consistent with all transitions being dipole: The data also uniquely determine the ground-state and excited-state spins of the scattering nucleus if a dipole transition is assumed.

While this analysis is simple and most encouraging, there is evidence[17,18] that some of the transitions excited with capture $\gamma$ rays are magnetic dipole $M1$ and also that some of the excited states decay with rather large branching ratios through mixtures of $M1$ and $E2$ radiation to lower-lying levels.[17] Thus, the possibility of an excitation of the level with mixed $M1$-$E2$ radiation cannot be ignored. However, such a possibility with its adjustable value $\delta$ for the mixing ratio widens considerably the range of $J_0$ and $J_1$ values that are compatible with the experimental data since now (with exceptions to be noted below):

$$W(\theta) = 1 + (1+\delta^2)^{-2} A_2^2(J_0, J_1, L, \delta) P_2(\cos\theta).$$

Using this more complex relation, the values of $J_0$, $J_1$, and $\delta$ giving $A_2^2$ values in agreement with the experimental parameters $\alpha \pm \Delta\alpha$ were calculated; they are listed in Table III. For several cases it has been noted in Table III that there are "many values possible" for $\delta$. These cases correspond to spin sequences such that a $P_4(\cos\theta)$ term is required in the theoretical expression for $W(\theta)$. The accuracy of the experimental data is insufficient to determine the coefficient of a $P_4(\cos\theta)$ term with a precision that will limit significantly the range of $\delta$ values that are compatible with the experimental data. Thus, the $\alpha$ values are not listed for these cases and the "many values possible" notation is used.

In summary then, all scattering data are consistent with pure dipole transitions (see Table II). However, for four cases Cd, Sn, Hg, and $^{205}$Tl, a limited number of mixtures of dipole-quadrupole radiation will also reproduce the data. Finally there is one Hg isotope and the $^{209}$Bi nucleus where the data are not sufficiently accurate to determine possible $\delta$ values.

[17] J. A. McIntyre and V. E. Michalk, Bull. Am. Phys. Soc. **12,** 1205 (1967); and data (to be published).
[18] R. Moreh and M. Friedman, Phys. Letters **26B,** 579 (1968).

TABLE II. Experiment compared to theory assuming a pure dipole transition.

| $J_1$ | $J_0$ | $A_2^2(J_0, J_1, L=1)$ (Theoretical) | $^{209}$Bi (7.149 MeV) | $^{209}$Bi (7.416 MeV) | $^{208}$Pb | $^{205}$Tl | Hg | Sn | Cd | $^{90}$Zr |
|---|---|---|---|---|---|---|---|---|---|---|
| | | | | | $\alpha \pm \Delta\alpha$ (Experimental) | | | | | |
| 1 | 0 | 0.500 | | | 0.485±0.026 | | 0.48±0.11 | 0.490±0.095 | **0.488±0.034** | **0.489±0.027** |
| 1/2 | 1/2 | 0.000 | | | | | 0.48±0.11 | 0.490±0.095 | 0.488±0.034 | |
| 3/2 | 1/2 | 0.250 | | | | 0.0017±0.0110 | 0.48±0.11 | 0.490±0.095 | 0.488±0.034 | |
| 1/2 | 3/2 | 0.000 | | | | 0.0017±0.0110 | 0.48±0.11 | | | |
| 3/2 | 3/2 | 0.160 | | | | | 0.48±0.11 | | | |
| 5/2 | 3/2 | 0.140 | | | | | 0.48±0.11 | | | |
| 7/2 | 9/2 | 0.024 | 0.184±0.074 | 0.195±0.033 | | | | | | |
| 9/2 | 9/2 | 0.194 | **0.184±0.074** | **0.195±0.033** | | | | | | |
| 11/2 | 9/2 | 0.083 | 0.184±0.074 | 0.195±0.033 | | | | | | |

TABLE III. Values of $J_0$, $J_1$, and δ compatible with experiment if a mixed dipole-quadrupole transition is assumed.

| ⁹⁰Zr | Cd | Sn | Hg | ²⁰⁵Tl | ²⁰⁸Pb | ²⁰⁹Bi (7.416 MeV) | ²⁰⁹Bi (7.149 MeV) | $J_0$ | $J_1$ |
|---|---|---|---|---|---|---|---|---|---|
| | | | δ±Δδ | | | | | | |
| | −1.319±0.044 | −1.32±0.12 | −1.33±0.14 | −3.73±0.63 | | | | 1/2 | 3/2 |
| | −0.126±0.016 | −0.127±0.045 | −0.122±0.056 | −0.268±0.056 | | | | 1/2 | 3/2 |
| | 7.95±0.93 | 7.9±2.6 | 8.3±2.9 | | | | | 1/2 | 3/2 |
| | 0.759±0.025 | 0.760±0.070 | 0.753±0.090 | | | | | 1/2 | 3/2 |
| | | | 0.211±0.022 | | | | | 3/2 | 3/2 |
| | | | 2.01±0.10 | | | | | 3/2 | 3/2 |
| | | | Many values possible | | | | | 3/2 | 3/2 |
| | | | | | | | | 3/2 | 5/2 |
| | | | | | | Many values possible | Many values possible | 9/2 | 7/2 |
| | | | | | | Many values possible | Many values possible | 9/2 | 9/2 |
| | | | | | | Many values possible | Many values possible | 9/2 | 11/2 |

Of course, it is possible to pursue further the multipole expansion. However, in the absence of evidence for a need for higher-order terms there is no purpose in extending the calculations further.

In addition to the above work, a ninth level, reported in the literature,[13] (the 7.16-MeV neutron-capture γ ray from Cu scattered by Tl) was also studied; however, it could not be found. Its scattering signal was less than 1% that of the 7.277-MeV Fe γ ray scattered by Pb.[19]

## B. Scattering Measurements

The absolute scattering measurements were made at $\theta=90°$. The detector subtended an angle of 8° in the scattering plane.

The main problem in the scattering measurement is to measure accurately all of the quantities appearing in the yield expression of Eq. (10) and its associated equations, Eqs. (11), (12), and (16). Some measurements are easily made such as those of temperature; the geometrical quantities, $\alpha$, $\beta$, $\theta$, and $x_0$; and $n$, the density of the resonant nuclei in the scatterer. Others are already known such as $W(\theta)$, the measurement of which was described in Sec. IV A and the energy of the γ rays[20] for determining $\lambda$. More difficult were the measurements of $d\Omega$, $\eta$, and $N_0$. The selection of the values used for $J_0$ and $J_1$ will be discussed in Sec. V A.

The solid angle subtended at the target by the entrance face of the NaI(Tl) detector must be modified[21] by a penetration factor which gives the "effective solid angle" $d\Omega$. The product $\eta N_0$ (detector efficiency multiplied by beam intensity) was measured by placing the NaI(Tl) detector in the γ-ray beam and obtaining a pulse-height spectrum. Since, in many cases, the γ ray responsible for the resonance scattering could not be isolated in the neutron-capture γ-ray NaI(Tl) spectrum, it was necessary to measure the intensity of the highest-energy γ ray in the spectrum and then multiply this intensity by (1) the published[20] intensity ratio between the desired γ ray and the highest-energy γ ray and (2) the detection-efficiency ratio[15] for the γ rays at the two energies. By making appropriate geometrical corrections involving the areas of the entrance face of the NaI(Tl) detector and the target intercepting the beam, the quantity $\eta N_0$ was determined.

The error assigned to the quantity $\eta N_0$ was ±20% for all cases except for Se. This assignment was made on the basis of discrepancies between the intensity ratios of Groshev et al.[20] and those measured more recently for ⁶⁰Co by Shera and Hafemeister[22] and for Cu by Bolotin.[23] For the remaining case of the Se source, because of lack

[19] This negative result has been confirmed. G. Ben-David, (private communication).

[20] L. V. Groshev, V. N. Lutsenko, A. M. Demidov, and V. I. Pelekov, Atlas of Gamma Spectra from Radiative Capture of Thermal Neutrons (Pergamon Press, Inc., New York, 1959).

[21] E. Hayward and E. G. Fuller, Phys. Rev. 106, 991 (1957).

[22] E. B. Shera and D. W. Hafemeister, Phys. Rev. 150, 894 (1966).

[23] H. H. Bolotin (private communication from L. M. Bollinger).

TABLE IV. Intensity ratios used.

| (Source, scatterer) | γ ray measured in direct beam | | γ ray resonantly scattered | | Reference |
| --- | --- | --- | --- | --- | --- |
| | Energy (MeV) | Intensity % | Energy (MeV) | Intensity % | |
| (Fe, Pb) | 9.298 | 3.3 | 7.277 | 5.3 | a |
| (Se, Zr) | 9.882 | 1.0 | 8.496 | 0.2 | b |
| (Fe, Tl) | 9.298 | 3.3 | 7.647 | 21.5 | a |
| (Se, Bi) | 9.882 | 1.0 | 7.416 | 2.2 | b |

[a] L. V. Groshev, A. M. Demidov, G. A. Kotelnikov, and V. N. Lutsenko, Nucl. Phys. **58**, 465 (1964).

[b] L. V. Groshev, V. N. Lutsenko, A. M. Demidov, and V. I. Pelekov, *Atlas of Gamma Spectra from Radiative Capture of Thermal Neutrons* (Pergamon Press, Inc., New York, 1959).

of other information, the intensity ratio was taken from the work of Kinsey and Bartholomew[24] whose intensity values for other elements differ from those of Groshev *et al.*[20] by as much as $\pm 40\%$. Since these intensity ratios are presently being measured more accurately at a number of laboratories we tabulate the intensity ratios used in our calculations in Table IV; when better ratios are published they can then be used to determine better values of $\eta N_0$. These new values of $\eta N_0$ can then be inserted in Eq. (10) to calculate better values of $\Gamma$, $\Gamma_0$, and $\epsilon$. Since the absorption and temperature experiments (which determine, respectively, to a first approximation, $\Gamma_0$ and $\epsilon$) are independent of $\eta N_0$, the main effect of a change in $\eta N_0$ is to change the value determined for $\Gamma$. Referring to Eq. (17), the approximate expression for Eq. (10), it is seen that the value found for $\Gamma$ will be proportional to the value used for $\eta N_0$ since $Y$, the experimental quantity, remains unchanged.

The yield for the scattering measurement was determined in the same manner as that used for the angular-

distribution measurements of Sec. IV A, energy spectra similar to those in Figs. 5 and 6 being obtained. Such scattering yields were obtained for four different scatterers. These yields were inserted into Eq. (10) and a search made with the IBM 7094 computer to find compatible values of $\Gamma$, $\Gamma_0$, and $\epsilon$. The search was made by selecting a value of $\Gamma_0/\Gamma = 1$ and then varying $\Gamma_0$ and $\epsilon$ for each scatterer studied. A curve in the $\Gamma_0 - \epsilon$ plane was thereby generated which satisfied the result of the scattering experiment. Such a curve for a $^{208}$Pb scatterer in an Fe beam is shown in Fig. 8. A second curve for $\Gamma_0/\Gamma = \frac{1}{2}$ is also plotted.

## C. Absorption Measurements

In these measurements, scattering experiments were made using various thicknesses $t$ for the absorber placed in the beam. Data, such as those shown in Fig. 9, were obtained for each absorber studied. Here, an absolute measurement was not necessary so that the uncertainty introduced by the determination of $\eta N_0$ into the scattering measurement of Sec. IV B is no longer present.

Since there are more than three points in Fig. 9, the determination of $\Gamma$, $\Gamma_0$, $\epsilon$, was made through a least-
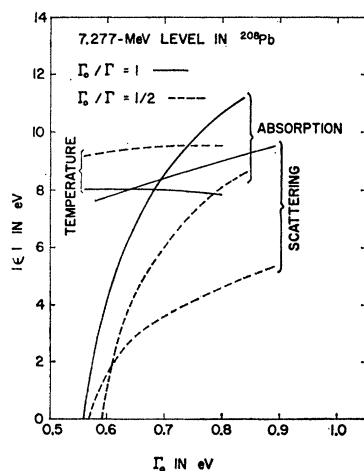


Fig. 8. The results of the analysis of the three experiments: (a) self-absorption, (b) scattering, and (c) temperature variation for different ratios for $\Gamma_0/\Gamma$ plotted in $\Gamma_0 - \epsilon$ plane. Data are for the 7.277-MeV level in $^{208}$Pb.

[24] B. B. Kinsey and G. A. Bartholomew, Can. J. Phys. **31**, 537 (1953).
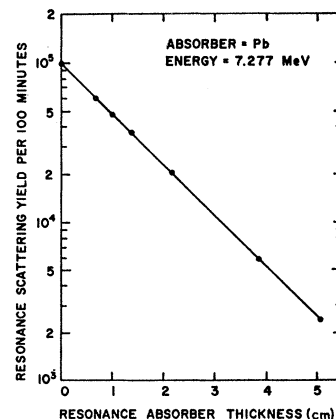


Fig. 9. A plot of resonant scattering yield versus absorber thickness for the 7.277-MeV level in Pb. The experimental errors are no larger than the points shown in the figure.

TABLE V. Summary of energy-level parameters.

| Element | $^{90}$Zr | Cd | Sn | Hg | $^{205}$Tl | $^{208}$Pb | $^{209}$Bi | $^{209}$Bi |
|---|---|---|---|---|---|---|---|---|
| Level energy (MeV) | 8.496[a] | 6.485[b] | 6.988[c] | 4.906[b] | 7.647[d] | 7.277[e] | 7.416[a] | 7.149[a] |
| γ ray source | Se | Co | Cu | Co | Fe | Fe | Se | Ti |
| $J_0 \to J_1$ | $0\to1$ | $0\to1$ | $0\to1$ | $0\to1$ | $1/2\to1/2$ | $0\to1$ | $9/2\to7/2$ | $9/2\to7/2$ |
|  |  | $(1/2\to3/2)$ | $(1/2\to3/2)$ | $3/2\to5/2$ | $(1/2\to3/2)$ |  | $9/2\to9/2$ | $9/2\to9/2$ |
|  |  |  |  | $(1/2\to3/2)$ |  |  | $9/2\to11/2$ | $9/2\to11/2$ |
|  |  |  |  | $(3/2\to3/2)$ |  |  |  |  |
| $\Gamma_0/\Gamma$ | $0.8\pm0.2$ |  |  |  | $0.85\pm0.17^f$ | $0.95^{+0.06}_{-0.17}$ | $0.6\pm0.2$ |  |
| $\Gamma_0$ (eV) | $1.68\pm0.02$ |  |  |  | $1.0^f$ | $0.68\pm0.03$ | $0.14\pm0.09$ |  |
| $\epsilon$ (eV) | $5.60\pm0.15$ |  |  |  | $11.5\pm0.2^f$ | $8.00\pm0.14$ | $3.4\pm1.6$ |  |

a L. V. Groshev, V. N. Lutsenko, A. M. Demidov, and V. I. Polekov, Atlas of Gamma Spectra from Radiative Capture of Thermal Neutrons (Pergamon Press, Inc., New York, 1959).
b E. B. Shera and D. W. Hafemeister, Phys. Rev. 150, 894 (1966).
c H. H. Bolotin (private communication from L. M. Bollinger).
d R. Moreh and G. Ben-Yaacov, Nuclear Research Center—Negev Report, NRCN-180, 1967, (unpublished).
e L. V. Groshev, A. M. Demidov, G. A. Kotelnikov, and V. N. Lutsenko, Nucl. Phys. 58, 465 (1964); G. T. Ewan and A. J. Tavendale, Nucl. Instr. Methods 26, 183 (1964).
f See Ref. 24a.

squares fit to the data. A plot of the curves in the $\Gamma_0-\epsilon$ plane determined by these fits for $\Gamma_0/\Gamma=1$ and $\Gamma_0/\Gamma=\frac{1}{2}$ is given in Fig. 8. Satisfactory values for $\chi^2$ were obtained along the curves plotted.

The accuracy of the resonance-absorption measurement is determined almost entirely by the accuracy of the published[8] nonresonance-absorption coefficients. (The geometry of the beam and absorber was sufficiently well defined so that these tabulated values could be used.) An estimate of the accuracy of the resonance-absorption measurement can be made in the following way. As seen in Fig. 9, the absorption curve is exponential so that the yield can be expressed as

$$Y(t) = C \exp(-\mu_0 t), \qquad (21)$$

where

$$\mu_0 = \mu_r + \mu \qquad (22)$$

and $C$ is a normalizing constant. Here, $\mu_r$ is the absorption coefficient introduced by the resonance excitation, while $\mu$ is the nonresonance-absorption coefficient. The quantity $\mu_0$ was then obtained by making a least-squares fit of Eq. (21) to the experimental data in Fig. 9. The value of $\mu$ was obtained from tables.[8] The published uncertainties for $\mu$ are in the 2% range. Thus, the percent error in the determination of $\mu_r$ is $2\mu/\mu_r$ which becomes large for $\mu\gg\mu_r$. Since $\Gamma_0$ is approximately proportional to $\mu_r$ [compare Eqs. (21) and (22) with Eq. (17)] the percent error in the value of $\Gamma_0$ is the same as that for $\mu_r$.

It should be noted here that a considerable improvement can now be made in the determination of $\mu$ using Ge(Li) detectors; such measurements are clearly important for utilizing the absorption method in studying the resonance fluorescence process.

### D. Temperature-Variation Measurements

Scattering-yield measurements were made at room temperature and at liquid-nitrogen temperature (78°K) and their ratio evaluated. A calculation was then made using Eq. (10) to determine yields at the two different temperatures (see Fig. 8) such that the calculated yield ratio gave the experimental value. Lines in the $\Gamma_0-\epsilon$ plane were then determined for $\Gamma_0/\Gamma=1$ and $\Gamma_0/\Gamma=\frac{1}{2}$ for these conditions. Since a ratio of the yields was calculated, the product $\eta N_0$ cancels out. Thus, the chief source of error is introduced through the determination of the yield from the pulse-height distribution spectrum.

### E. Determination of Γ, Γ₀, and ε

Inspection of Fig. 8 shows that the scattering measurement is the measurement most sensitive to a change in the ratio $\Gamma_0/\Gamma$. Thus, the intersection of the absorption and temperature lines for $\Gamma_0/\Gamma=1$ was used to obtain a first approximation for $\Gamma_0$ and $\epsilon$. With these values of $\Gamma_0$ and $\epsilon$, the value of $\Gamma_0/\Gamma$ was found, which could give the experimental scattering yield in Eq. (10). This new value of $\Gamma_0/\Gamma$ was then used to find new values

for $\Gamma_0$ and $\epsilon$ which would satisfy the absorption and temperature experiments, respectively. The iteration was continued until a set of $\Gamma_0/\Gamma$, $\Gamma_0$, and $\epsilon$ values consistent with all three experiments was obtained.

The uncertainties in the $\Gamma_0/\Gamma$, $\Gamma_0$, and $\epsilon$ values were found as follows. For each of the three experiments there was an uncertainty in the yield $Y$ as well as in certain parameters such as $\mu$ or $\eta N_0$. Corresponding to these uncertainties there were corresponding uncertainties in $\Gamma_0/\Gamma$, $\Gamma_0$, and $\epsilon$ for each experiment. The final uncertainties selected for $\Gamma_0/\Gamma$, $\Gamma_0$, and $\epsilon$ were the smallest values found among those calculated for the three different experiments. Thus, for the Fe-Pb experiment, illustrated in Fig. 8, the scattering experiment gave $0.95_{-0.17}^{+0.05}$ for $\Gamma_0/\Gamma$, $0.68\pm0.11$ eV for $\Gamma_0$, and $8.0\pm1.0$ eV for $\epsilon$. The absorption experiment gave $0.95_{-0.84}^{+0.05}$ for $\Gamma_0/\Gamma$, $0.68\pm0.03$ for $\Gamma_0$, and $8.0\pm6.3$ eV for $\epsilon$. The temperature experiment gave $0.95_{-0.26}^{+0.05}$ for $\Gamma_0/\Gamma$, $0.68\pm0.28$ eV for $\Gamma_0$, and $8.00\pm0.13$ eV for $\epsilon$. The final values are, therefore, $0.95_{-0.17}^{+0.05}$ for $\Gamma_0/\Gamma$, $0.68\pm0.03$ eV for $\Gamma_0$, and $8.00\pm0.13$ eV for $\epsilon$. These values are listed in Table V. A similar analysis was performed for the other energy levels studied; the parameters determined for these levels are listed also in Table V.

It is seen from the values quoted above that the scattering measurement determines the value of $\Gamma_0/\Gamma$, the absorption measurement the value of $\Gamma_0$, and the temperature measurement the value of $\epsilon$. However, if the resonance-absorption coefficient is much smaller than the nonresonance-absorption coefficient, then the tabulated[8] 2% error in the nonresonance coefficient introduces a large error in the resonance coefficient and hence in $\Gamma_0$ (see Sec. IV C). This was the case for the 7.416-MeV level in $^{209}$Bi where the error in $\Gamma_0$ is 55%. Under such circumstances, the usual scattering measurement will give a better value of $\Gamma_0$. However, the intensity of the 7.416-MeV $\gamma$-ray beam is not known to an accuracy better than 40% because of the uncertainty in the relative intensities of the neutron-capture $\gamma$ rays.[20] Hence, for this case, the scattering measurement cannot be used to give a significantly better value for $\Gamma_0$.

# V. DISCUSSION OF RESULTS

## A. Comments on the Individual Transitions

### 1. 8.496-MeV Level in Zr

There are five natural isotopes of Zr. Three of these, $^{91}$Zr, $^{94}$Zr, and $^{96}$Zr have neutron binding energies less than the energy of the level excited in the Zr nucleus. Since $\gamma$-ray emission from a level above the neutron threshold would be unlikely[24a] because of the competing neutron emission, these three nuclei can be excluded from the resonance-fluorescence process for excitation of the 8.496-MeV level. Reference to Table II shows that the angular distribution for Zr is consistent with $J_0=0$ and $J_1=1$ which applies to both $^{90}$Zr and $^{92}$Zr. It was found, however, that the three experiments on scattering, absorption, and temperature variation gave consistent results only for $^{90}$Zr because of the large difference in abundance (51 and 17%) between $^{90}$Zr and $^{92}$Zr. Thus, the 8.496-MeV level belongs to the $^{90}$Zr nucleus. The parameters measured for this level are all listed in Table V. Other work[17] has shown that the NaI(Tl) peaks used as the primary experimental data include only elastic scattering from the 8.496-MeV level as assumed in the analysis and interpretation of the experimental results.

### 2. 6.485-MeV Level in Cd

There are eight natural isotopes of Cd, six with spin zero and two with spin $\frac{1}{2}$. All have neutron binding energies greater than the excitation energy of the 6.485-MeV level and so cannot be ruled out on the basis of neutron emission from the excited level. Reference to Table II shows that the angular-distribution measurement is consistent with the nucleus having zero spin. However, it is also possible for a spin-$\frac{1}{2}$ nucleus to be excited to a spin-$\frac{3}{2}$ level with just the right amount of dipole-quadrupole mixing to reproduce the experimental data. The values of $\delta$, the mixing ratio, which are consistent with the $\frac{1}{2}\to\frac{3}{2}\to\frac{1}{2}$ transition and the experimental data are shown in Table III. Because of the good quality of the angular-distribution data, only a small range of $\delta$ (on the average 6%) is consistent with the data. It would appear unlikely that, considering the small range of $\delta$ allowed, the value of $\delta$ would be just such as to mimic the pure dipole $0\to1\to0$ transition. We conclude, therefore, that the transition is very likely a $0\to1\to0$ one. The spins $J_0\to J_1$ are listed, therefore, in Table V as $0\to1$ and $(\frac{1}{2}\to\frac{3}{2})$ the less likely values being in parentheses.

---

[24a] *Note added in proof.* In a private communication, Dr. R. Moreh has informed us that through decay studies of the excited level and work with separated isotopes, he has shown that the 7.647-MeV excitation in Tl occurs in $^{205}$Tl and not in $^{203}$Tl even though the level is $113\pm7$ keV above the neutron separation [J. H. E. Mattauch, W. Thiele, and A. H. Wapstra, Nucl. Phys. **67**, 32 (1965)]. This information shows that the arguments ruling

out isotopes on the basis of the neutron binding energy are invalid. Thus, $^{91}$Zr, $^{94}$Zr, and $^{96}$Zr cannot be eliminated on this basis. However, $^{92}$Zr was ruled out because its low abundance (17%) led to inconsistencies among other data. It is also possible to eliminate $^{91}$Zr, $^{94}$Zr, and $^{96}$Zr on this basis, leaving $^{90}$Zr still as the isotope being excited. Again, for tin, $^{117}$Sn and $^{119}$Sn can no longer be eliminated using the neutron-binding-energy argument. However, the angular-distribution measurement favors the even-even (spin 0) nuclei. The change of the Tl isotope from 203 to 205 affects the values calculated from $\Gamma_0$, $\Gamma_0/\Gamma$, and $\epsilon$. Without a complete computer recalculation, the approximate adjustments of these values can be made. The value for $\Gamma_0$ depends primarily on the absorption measurement and the absorption coefficient $\mu_r$ and is thus inversely proportional to $n$, the number of nuclei per cm$^3$, and hence the nuclear abundance [see Eqs. (22) and (23) and subsequent discussion]. Thus, $\Gamma_0$ is reduced from $2.42\pm0.15$ eV as calculated by the computer to 1.0 eV. In the scattering experiment, the scattering yield is proportional, naturally, to the abundance. However, the yield is also proportional to $\Gamma_0(\Gamma_0/\Gamma)$. Thus, the increase in abundance is canceled by the decrease in $\Gamma_0$ just discussed and the value of $\Gamma_0/\Gamma$ is unchanged. For the temperature variation experiment, the result depends, to a first approximation, only on line shapes and not on abundance. Thus, to a first approximation, $\epsilon$ will also remain unchanged.

TABLE VI. Comparison of level parameters for the 7.277-MeV level in lead.

| Reference | $\Gamma_0/\Gamma$ | $\Gamma_0$ (eV) | $\epsilon$ (eV) |
|-----------|-------------------|-----------------|-----------------|
| a | 0.70±0.35 | 0.80±0.08 | 4.8±0.4 |
| b | | 0.1≤$\Gamma_0$≤4 | 26 |
| c | ~1 | 0.8±0.03 | 8.5±0.5 |
| d | | | 6.5±1 |
| e | 0.72±0.13 | 0.86±0.06 | 5.0±0.5 |
| f | 1 (assumed) | 0.7±0.2 | |
| g | | 0.56±0.08 | 7.5±0.6 |
| h | $0.95_{-0.17}^{+0.05}$ | 0.68±0.03 | 8.00±0.14 |

a H. H. Fleischmann and F. W. Stanek, Z. Physik 175, 172 (1963).
b C. S. Young and D. J. Donahue, Phys. Rev. 132, 1724 (1963).
c B. Arad, G. Ben-David, I. Pelah, and Y. Schlesinger, Phys. Rev. 133, B684 (1964).
d B. Arad, G. Ben-David, and Y. Schlesinger, Phys. Rev. 136, B370 (1964).
e M. Giannini, P. Oliva, D. Prosperi, and S. Sciuti, Nucl. Phys. 65, 344 (1065).
f J. A. McIntyre and J. D. Randall, Phys. Letters 17, 137 (1965).
g C. J. Kapadia, V. E. Michalk, and J. A. McIntyre, Nucl. Instr. Methods 59, 197 (1968).
h This work.

There is also the possibility that in addition to the elastic scattering being studied, inelastic or other resonance scattering processes will occur which will not be recognized because of the poor energy resolution of the NaI(Tl) detector. Recent work[17] with much better resolution, using a Ge(Li) detector, has shown that the intensity of the scattering other than elastic is small enough not to significantly affect the data published here. However, the Ge(Li) work did show that a second neutron-capture $\gamma$ ray at 6.278 MeV was also being scattered. Since its angular distribution was found to be the same as that for the 6.485-MeV $\gamma$ ray, it did not introduce any distortion in the angular-distribution measurement.

### 3. 6.988-MeV Level in Sn

There are ten natural isotopes of Sn, seven with spin zero and three with spin $\frac{1}{2}$. Two of these, $^{117}$Sn and $^{119}$Sn, have a neutron binding energy less than that of the 6.988-MeV excitation and so can be ruled out[24a] (see Sec. V A1). Reference to Tables II and III shows that, as for the Cd case just discussed, (1) a pure dipole transition from a spin-zero ground state is consistent with the data, and (2) a limited range of $\delta$ (about 20%) is also consistent with the data. The spins are listed in Table V, therefore, as 0→1 and ($\frac{1}{2}$→$\frac{3}{2}$).

It should also be noted here that the value for $\alpha$ shown in Table II is in disagreement with a value reported in the literature.[25] These authors report a value of $\alpha$=0.24±0.04 while the experimental result listed in Table II has a value of 0.490±0.095.

25 M. Giannini, P. Oliva, D. Prosperi, and G. Toumbev, Nucl. Phys. A101, 145 (1967).

Again, as with Cd, there is the possibility of inelastic and other elastic scattering under the NaI(Tl) peaks. However, recent measurements[17] with a Ge(Li) detector have shown that there is no detectable amount of such extraneous scattering. Thus, the scattering measured here with the NaI(Tl) detector represents only elastic scattering of the 6.988-MeV $\gamma$ ray.

### 4. 4.906-MeV Level in Hg

There are seven natural isotopes of Hg, five with spin-zero ground state, one with spin $\frac{1}{2}$, and one with spin $\frac{3}{2}$. All have neutron binding energies greater than 4.906 MeV and so are possible isotopes for excitation. Reference to Tables II and III shows that (1) a pure dipole transition from the ground state of a spin-zero isotope is consistent with the data, and (2) a limited range of $\delta$ (about 25%) is also consistent with the data. In addition, if the transition is in the Hg isotope with spin $\frac{3}{2}$, a large range of $\delta$ values is possible for the $\frac{3}{2}$→$\frac{5}{2}$→$\frac{3}{2}$ transition. The spins are listed in Table V therefore, as 0→1, $\frac{3}{2}$→$\frac{5}{2}$, and ($\frac{1}{2}$→$\frac{3}{2}$) for the $J_0$→$J_1$ transition, the parentheses indicating the less likely transition.

No data have yet been taken with the Ge(Li) detector for the Hg resonance scattering. Thus, the inelastic or other extraneous contribution to the scattering is not well determined for this case.

### 5. 7.647-MeV Level in Tl

There are two natural isotopes of Tl, with $A=203$ and 205. The neutron binding energy is too small for $^{205}$Tl to be the correct isotope.[24a] Reference to Tables II and III shows that the $\frac{1}{2}$→$\frac{1}{2}$→$\frac{1}{2}$ dipole transition is consistent with the data. For a limited range of $\delta$ (about 20%) the $\frac{1}{2}$→$\frac{3}{2}$→$\frac{1}{2}$ transition is also possible. Applying the arguments presented above, the spins are listed in Table V as $\frac{1}{2}$→$\frac{1}{2}$ and ($\frac{1}{2}$→$\frac{3}{2}$).

Recently, this scattering process has been studied by Moreh and Ben-Yaacov[26] who used a Ge(Li) detector which showed that only the elastic scattering would appear under the NaI(Tl) peaks. Thus, not only the angular-distribution results but also the values quoted in Table V for $\Gamma_0/\Gamma$, $\Gamma_0$, and $\epsilon$ are free from error introduced by processes other than elastic scattering to the 7.647-MeV level.

Moreh and Ben-Yaacov also found $\alpha=0$ from their angular-distribution measurement in agreement with the results quoted here. It should be remarked here also that the value[24a] for $\Gamma_0$ listed in Table V, 2.42±0.15 eV is in agreement with another measurement[27] where a value of 2.2 eV was obtained.

### 6. 7.277-MeV Level in Pb

There are three natural isotopes of Pb: 206, 207, and 208. It has been shown previously[28] that the transition

26 R. Moreh and G. Ben-Yaacov, Nuclear Research Center—Negev Report, NRCN-180, 1967 (unpublished).
27 B. Arad (private communication of work of J. Balderman).
28 C. S. Young and D. J. Donahue, Phys. Rev. 132, 1724 (1963).

occurs in $^{208}$Pb. The values for $\Gamma_0/\Gamma$, $\Gamma_0$, and $\epsilon$ have been measured many times. The results listed in Table V are in agreement with most of the previous measurements which are exhibited in Table VI.

### 7. 7.416-MeV Level in $^{209}$Bi

There is only one isotope of Bi. If a pure dipole transition was assumed a fit to the data could be obtained only for the $\frac{9}{2}\to\frac{9}{2}\to\frac{9}{2}$ transition (see Table II). However, with the large ground-state spin of $\frac{9}{2}$ it is difficult to distinguish between angular distributions corresponding to different values of $\delta$ as indicated in Table III. Thus, all three possible transitions are listed in Table V. It should be noted that, because of the uncertainty in $J_1$ it is not possible to insert a precise value for the statistical factor $2J_1+1$ into the analysis of the results of the scattering and absorption measurements. Since $\frac{7}{2}<J_1<\frac{11}{2}$, $2J_1+1$ has a value $10\pm2$ and the uncertainty in the values of $\Gamma_0/\Gamma$ and $\Gamma_0$ must be increased accordingly. These increases are included in the errors listed in Table V.

For this level no work has been reported using Ge(Li) detectors; however, the first excited state of $^{209}$Bi is at 0.9 MeV so that inelastic scattering cannot be confused with the elastic scattering process. (It is assumed that the high-energy $\gamma$ ray in a cascade is emitted first because of the energy dependence of the probability of $\gamma$-ray emission.)

### 8. 7.149-MeV Level in $^{209}$Bi

The same comments apply here for the spins as to the other level in Bi discussed above.

### B. General Comments

The experimental angular-distribution data $W(\theta)$ are presented through the $\alpha$ values listed in Table II where $W(\theta)=1+\alpha P_2(\cos\theta)$. Other results are summarized in Table V.

There are several features of interest in the results of Table V. First, for two of the eight cases studied, the transitions are pure dipole ($^{90}$Zr and $^{208}$Pb), three are most likely pure dipole (Cd, Sn, and $^{203}$Tl) while three (Hg and both Bi cases) are also consistent with this

result. Second, the values found for $\Gamma_0$ are large compared to values found in transitions from levels near the neutron threshold. Usually the magnitude of $\Gamma_0$ is in the 0.1-eV range, as determined from the study of levels populated by neutron capture,[9] while the $\Gamma_0$ values in Table V range from 0.14 to 1.0 eV.

These experimental results are not surprising since the experimental cases studied are just those where the resonance scattering cross section is large, i.e., where $\Gamma_0$ is large. Since $\Gamma_0$ is expected usually to be largest for dipole transitions the dominance of such transitions would not be unexpected.

Again, due to experimental bias, values of $\Gamma_0/\Gamma$ are found to be near unity (see Table V). Nevertheless, even for the nuclei studied with their large values of $\Gamma_0$, there are cases where transitions to levels other than the ground state are evident (see Table I). The study of these transitions will give information about the spins and linewidths of low-lying nuclear levels. Investigations of such transitions have already been carried out by Min and Estes.[29]

## VI. CONCLUSIONS

Eight nuclear levels have been excited by the resonance fluorescence process in the 5–9-MeV energy region. The data are all consistent with a dipole excitation of the nuclear states; however, mixed dipole-quadrupole excitation is also possible in all but two cases. Further study of four of the levels gave linewidths $\Gamma_0$ for ground-state transitions which lie between 0.14 and 1.0 eV. The branching ratios $\Gamma_0/\Gamma$ for the levels studied range between 0.6 and 0.95.

## ACKNOWLEDGMENTS

[29] K. Min, Phys. Rev. **152**, 1062 (1966); G. P. Estes and K. Min, *ibid*. **154**, 1104 (1967).